
A Hitchhikers Guide to Fine-Grained Face Forgery Detection Using Common Sense Reasoning

Niki Maria Foteinopoulou¹ Enjie Ghorbel^{1,2} Djamila Aouada¹

¹CVI², SnT, University of Luxembourg

²Cristal Laboratory, National School of Computer Sciences, University of Manouba
`{niki.foteinopoulou, enjie.ghorbel, djamila.aouada}@uni.lu`

Abstract

Explainability in artificial intelligence is crucial for restoring trust, particularly in areas like face forgery detection, where viewers often struggle to distinguish between real and fabricated content. Vision and Large Language Models (VLLM) bridge computer vision and natural language, offering numerous applications driven by strong common-sense reasoning. Despite their success in various tasks, the potential of vision and language remains underexplored in face forgery detection, where they hold promise for enhancing explainability by leveraging the intrinsic reasoning capabilities of language to analyse fine-grained manipulation areas. As such, there is a need for a methodology that converts face forgery detection to a Visual Question Answering (VQA) task to systematically and fairly evaluate these capabilities. Previous efforts for unified benchmarks in deepfake detection have focused on the simpler binary task, overlooking evaluation protocols for fine-grained detection and text-generative models. We propose a multi-staged approach that diverges from the traditional binary decision paradigm to address this gap. In the first stage, we assess the models' performance on the binary task and their sensitivity to given instructions using several prompts. In the second stage, we delve deeper into fine-grained detection by identifying areas of manipulation in a multiple-choice VQA setting. In the third stage, we convert the fine-grained detection to an open-ended question and compare several matching strategies for the multi-label classification task. Finally, we qualitatively evaluate the fine-grained responses of the VLLMs included in the benchmark. We apply our benchmark to several popular models, providing a detailed comparison of binary, multiple-choice, and open-ended VQA evaluation across seven datasets. <https://nickyfot.github.io/hitchhikersguide.github.io/>

1 Introduction

Recent developments in deep generative modelling have resulted in hyper-realistic synthetic images/videos with no clear visible artefacts, making the viewers question whether they can still trust their eyes. Unfortunately, despite its relevance in a wide range of applications, such technology poses a threat to society as it can be used for malicious activities [16]. In a world where synthetic images of a person, known as deepfakes, can easily be generated, it becomes crucial to fight misinformation not only by identifying manipulated images/videos in an automated manner but also by explaining the decision behind this classification to reinstate trust in Artificial Intelligence.

Numerous successful works on deepfake detection have been proposed in the literature to tackle the risks of face forgery [37, 76, 52, 7, 80]. Existing methods primarily rely on deep binary classifiers, resulting in black-box models that predict whether an input is real or fake. Consequently, explaining why those predictions are being made is not straightforward. To handle this issue, a

few interpretable deepfake detection methods have been introduced by examining attention maps or weight activations [86, 71] to identify fine-grained areas of manipulation; however, these are based on a post-hoc analysis and thereby do not intrinsically incorporate an explainable mechanism. On the other hand, Vision Large Language Models (VLLMs) have emerged as a pioneering branch of generative Artificial Intelligence (AI), showcasing advancements in common sense reasoning and an inherent explainability that arises from the intrinsic nature of language [22]. They have demonstrated impressive capabilities in tasks such as Visual Question Answering (VQA) [47] and the generation of descriptive content for downstream applications [70], hence bridging the gap between vision-language understanding and contextual reasoning. However, despite these achievements, the explainable power of VLLMs remains under-explored in the field of deepfake detection, with only a handful of works exploring the vision and language capabilities for the binary classification of fake/real images [26, 8, 31, 69] all of which are evaluated on different benchmarks and metrics.

Explainable fine-grained detection –that is, identifying manipulation beyond the binary fake/real decision– in natural language is still in its infancy. However, as VLLM works for deepfake detection are expected to appear following the overwhelming success of foundation models in other tasks, two research questions need to be addressed: 1) *“To what extent can existing VLLMs detect deepfake images and what rationale supports the decision?”* and 2) *“How do we fairly and comprehensively evaluate VLLMs in the fine-grained task?”*. In deepfake detection, benchmarks have mainly focused on binary decisions and discriminative networks [81], making them unsuitable to answer these research questions. Indeed, they do not propose a unified method to match the generated responses to fine-grained categories. Similarly, existing benchmarks in Visual Question Answering (VQA) [19, 10] primarily address multi-class tasks, which may not be suitable for the multi-label nature of fine-grained deepfake detection as highlighted in [63].

In this work, our objective is to conduct a thorough quantitative and qualitative evaluation of VLLMs for the task of fine-grained deepfake detection in a systematic and scientific approach, employing a multi-stage protocol. In the first stage, we assess the models’ performance on the binary task using various prompts while also evaluating the model’s sensitivity to the provided instructions. In the second stage, we delve into fine-grained detection, aiming to identify areas of manipulation within a closed-form Visual Question Answering (VQA) framework, i.e. what areas from a given list are identified as manipulated. Subsequently, in the third stage, we extend our investigation by converting the fine-grained detection task into an open-ended question –that is, identifying areas without instructing the model to select from a list of categories. Here, as the task is a multi-label problem, we compare two matching strategies: a) using the cosine similarity between the generated text and ground truth labels and b) counting the occurrence of the class name in the generated text. Finally, we qualitatively evaluate the fine-grained responses generated by the VLLMs included in our benchmark, providing nuanced and new insights into their performance.

The main contributions of this work can be thus summarised as follows:

- We introduce a novel approach in deepfake detection by proposing a method to transform the discriminative task into a Visual Question Answering (VQA) multi-label problem. To the best of our knowledge, this is the first work to do so in the field of deepfake detection, offering a fresh perspective on explainability through fine-grained analysis.
- We establish a systematic, unified evaluation framework for current state-of-the-art (SOTA) VLLMs, facilitating consistent assessment across different models. This framework is designed to be extendable, ensuring fair and comprehensive comparisons with future models, thus promoting transparency and reproducibility in the evaluation process.
- Through extensive comparison and analysis of the tested models and an ensemble of models, our study yields new insights into the capabilities and limitations of VLLMs in the context of deepfake detection. We will use these insights to advance research in the domain and hope to inform future developments and optimisations in model design and evaluation strategies.

2 Related Work

DeepFake generation encompasses various forms of facial manipulation, including face reenactment [6, 1], face swapping [24, 45], and entirely generated face images [32, 68]. **Deepfake detection** algorithms classify samples as real or fake [7, 80, 76, 37], relying on artefacts left by manipulation methods, often analysed qualitatively for explainability [21, 89]. However, this qualitative analysis

happens on a secondary stage and primarily depends on human observers. While generative methods often use natural language instructions [54, 74, 58, 55, 77], explaining manipulations in natural language –a natural extension of the generation process to detection– is still an emerging area.

With the rise of VLLMs, recent works [8, 31, 69, 30, 72] explore vision and language for face forgery detection, primarily focusing on binary detection in a retrieval setting, with fewer [69, 52, 89] examining fine-grained areas usually as a secondary task. The latter have relied on generated pseudo-fake datasets to improve generalisation [69, 52, 89], which have a major drawback –that is, the use of pseudo-fake datasets hampers fair comparisons and does not reflect the current state-of-the-art in deepfake generation.

Several **VLLMs** foundation models [4, 15, 35, 44, 43], bridge the gap between vision and language. These are typically trained on very large datasets with general knowledge. As the computational and data resources needed to train VLLMs from scratch are very high, numerous works leverage the pre-trained networks in three main directions: a) exploring the latent feature space [14, 57] of vision and language, b) parameter efficient training in a downstream task [39, 73, 18] and c) evaluating foundation models in new domains [65, 75].

Benchmarks for classification tasks [19, 38, 2] in a VQA setting typically address the multi-class paradigm, which may not be appropriate for addressing explainability in DeepFake detection by adopting a multi-label fine-grained strategy, as several areas can be manipulated at once. A few preliminary works in DeepFake detection [3, 26] benchmark ChatGPT4¹ and Gemini²; however, these have primarily focused on the more straightforward binary task and did not explore the reasoning capabilities of VLLMs for fine-grained labels. Furthermore, both these works focused on VLLMs that are not open-sourced with limited information regarding their training set and architecture; thus, it is not possible to assess whether the benchmarks are, in fact, zero-shot or whether they have been trained on deepfake-related image-language pairs. Within DeepFake detection, the vast majority of benchmarking works [60, 65, 46, 81, 34] have focused on binary discriminative networks and are therefore not fit to evaluate the capabilities of generative models such as VLLM, particularly for fine-grained labels.

In a nutshell, the main novelty of this benchmark compared to previous works [19, 81, 38, 2, 60, 65, 46, 34] is threefold: 1) it converts the multi-label classification task of face forgery detection to a VQA task so that VLLM’s common sense reasoning capabilities can be evaluated, 2) it systematically and consistently assesses VLLM capabilities on nine binary and three fine-grained benchmarks and 3) is offering an open source and extendable framework for future zero-shot or task-specific VLLMs, that ensures a fair comparison.

3 Common Sense Reasoning for Face Forgery Detection

Preliminaries: We formalise the language generation process of VLLM architectures, akin to standard VQA models, where the model is prompted with an image and a query to produce an auto-regressive answer. Given an image $\mathbf{X}_v \in \mathbb{R}^{H \times W \times C}$ and a text prompt $\mathbf{X}_t \in \mathbb{R}^{L \times d}$ as input, a sentence ψ is generated represented as a sequence of word tokens. The generation can be represented by the function $p(\psi | \mathbf{X}_v, \mathbf{X}_t) = \prod_{j=0}^{|\psi|} p(\psi_j | \psi_{<j}, \mathbf{X}_v, \mathbf{X}_t)$, where $H \times W \times C$ represent the image dimension, L is the number of tokens, d is the embedding dimension, $\psi = (\psi_j)_{0 \leq j < |\psi|}$ is the generated sentence, and $|\cdot|$ the cardinality. In VQA tasks, the model response aims to match human annotations. This task differs from typical classification problems due to the diverse semantic nature of questions and answers in natural language. The evaluation protocol is outlined for the binary case in Section 3.1 and for open-ended evaluation and multiple-choice of fine-grained labels in Section 3.2. An overview of the proposed method is shown in Figure 1.

3.1 Binary Classification to VQA

In binary classification, the task is to predict whether the image sample is a product of face forgery. We create a benchmark to assess VLLM capability in binary Deepfake detection by transforming the discriminative task into a VQA problem. We consider only the positive category for each image \mathbf{X}_v

¹<https://openai.com/gpt-4>

²<https://gemini.google.com>

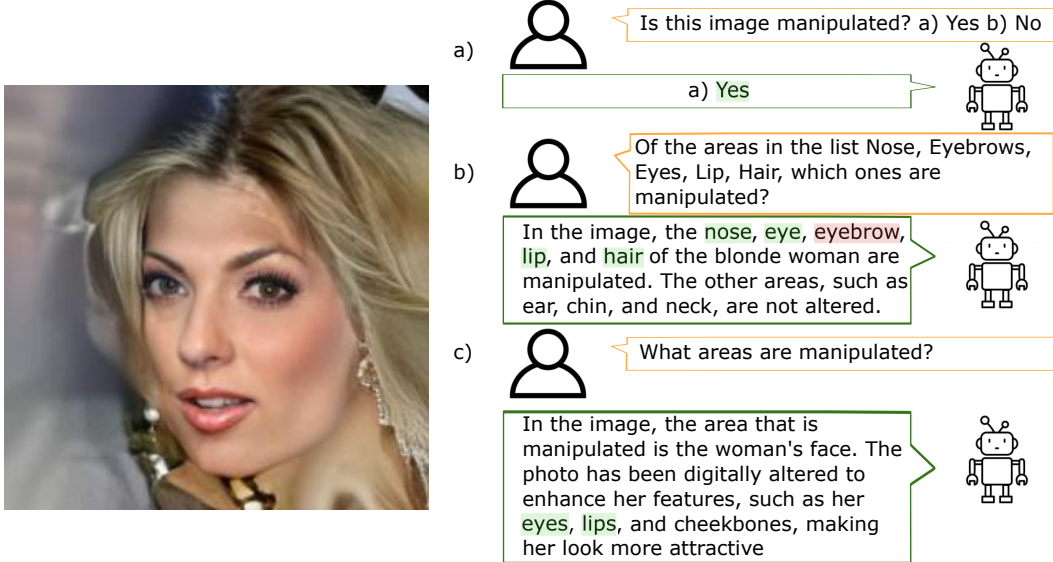


Figure 1: Overview of the proposed benchmarking method, using multiple stages to evaluate the performance of VLLMs in the context of deepfake detection. In the first stage (a), we assess the binary classification performance of VLLMs. In the second stage (b), we perform a fine-grained classification using multiple-choice instruction. In the third and final stage (c), we ask the model to identify fine-grained areas in open-ended VQA. The image example ³is a sample from the SeqDeepFake dataset [63], and responses are generated using Llava-1.5 [43]

to generate the relevant instruction; that is, we limit the prompt to identifying whether an image is a Deepfake and not whether it is a genuine sample. The prompt used is in the form:

$$\mathbf{X}_t = \text{“Is this image } [s_i] \text{ ? a) Yes b) No”} \quad (1)$$

where $s_i \in \mathcal{S}$ denotes a set of standard terms used to describe deep fakes in the English language. The synonyms are employed to assess the reasoning capabilities of each tested model by investigating whether the understanding of the model is robust to the given instruction.

3.2 Fine-Grained Labels:

Fine-grained labels typically refer to manipulation areas. Predicting them necessitates the use of multi-label classification, as multiple areas can be manipulated at once. Following the initial binary prompt, a follow-up prompt to explain what areas of manipulation are identified is given to the VLLM with the same image, as shown in Fig. 1. We propose using two versions of follow-up prompts, one as an open-ended question and one as a multiple-choice. Specifically, the open-ended follow-up prompt follows the template:

$$\mathbf{X}_t = \text{“What area of this image is } [s_i] \text{ ?”} \quad (2)$$

For the multiple-choice instruction, we follow the template:

$$\mathbf{X}_t = \text{“Of the areas in the list } [\text{cls}_0, \dots, \text{cls}_{|\mathcal{C}|}], \text{ which ones are } [s_i] \text{ ?”} \quad (3)$$

where $\text{cls}_i \in \mathcal{C}$ is the class name of the i -th class from the set of target classes \mathcal{C} .

3.3 Matching Strategies:

To evaluate the generated responses, we employ several matching methods depending on the task. The stricter one uses an *Exact Match (EM)* approach, that estimates whether the generated sentence

³Ground truth: Hair, Nose, Lip, Eye

ψ is exactly equal to the class name cls_i :

$$p(\hat{y}_i) = \begin{cases} 1 & \text{if } \psi \equiv \text{cls}_i \\ 0 & \text{if } \psi \neq \text{cls}_i \end{cases} \quad (4)$$

where \hat{y}_i is the prediction for the i -th class. In the given task, an answer is considered correct only if the model output exactly matches the class names or ‘Yes’/‘No’ in the binary case. As the responses tend to be longer for fine-grained classification and reflect reasoning in natural language for a multi-label problem, a more appropriate matching strategy is to consider a response correct if the class name is *Contained* in the response, as proposed by Xu *et al.* [75] – that is $p(\hat{y}_i) = 1$, if $\text{cls}_i \in \psi$ and 0 otherwise. We extend this to include synonyms of class names, as several ways exist to describe some areas (e.g. “Bangs” could also be described as “Hair”). Finally, we propose adapting the text-to-text score (*CLIP distance*) proposed by Conti *et al.* [14] for the multi-label task. This is done by using a sigmoid function over the cosine similarity matrix of the prediction embeddings and class name embeddings (obtained with a CLIP [59] text encoder), using an empirical temperature t of 0.5 so that $p(\hat{y}_i) = \sigma(\langle \psi, \text{cls}_i \rangle \cdot \frac{1}{t})$. The symbol $\langle \cdot, \cdot \rangle$ denotes the cosine similarity of the text embeddings and $\sigma(\cdot)$ is the sigmoid function.

4 Experimental Set-Up

4.1 Tested VLLMs

We select four open-source state-of-the-art VLLMs to be included in this benchmark; specifically, we include LlaVa-1.5 [43] (an improved version of the LlaVa architecture [44]), BLIP2 [35] and finally InstructBlip [15] with Flan-T5 and Flan-T5-xxl language generators [13]. Finally, for the binary task, we include the CLIP [59] performance as a baseline and compare it against an ensemble of BLIP2 [35] and LlaVa-1.5 [43] following the ensembling strategies for VQA tasks [5], and GPT4v as an upper bound⁴. Experiments using GPT4v are performed on a subset of 5k samples selected from each dataset and thus the results may be susceptible to some degree of bias from the sampling, which needs to be considered when comparing the models. The selection of the VLLM is guided by three factors. First, we select architectures with publicly available weights and training methods to ensure transparency and fairness in the evaluation. Second, we include methods that generate output in Natural Language rather than a set of features or classification predictions. Finally, we select methods that have achieved state-of-the-art performance on several zero-shot tasks. Additional model details, such as the number of parameters and pre-training information of the tested models, can be found in Appendix A.

4.2 Datasets

We evaluate the performance of our method on seven published challenging benchmarks and one pseudo-fake dataset; more specifically, seven datasets for binary detection and two for the fine-grained task. All are evaluated at the frame level, as in previous image works [79, 52, 49]. **FF++**: [60] consists of over 20k images of DeepFake images from 1000 videos, using four types of manipulation methods: Deepfakes, Face2Face, FaceSwap and NeuralTextures. The dataset is split into train, validation, and test with an 80%, 10%, and 10% split, respectively. **DFDC**: [17] is composed of 5k videos of real and manipulated faces split into 4,464 unique training clips and 780 unique test clips. **Celeb-DF**: [41] includes 590 original videos collected from YouTube with subjects of different ages, ethnic groups and genders, and 5639 corresponding manipulated videos. **WildDeepFake**: [88] is a challenging dataset for in-the-wild detection, which consists of 7,314 face sequences extracted from 707 videos that are collected completely from the internet. **StyleGAN**: Two sub-sets consist of curated images generated with StyleGAN3 [29] and StyleGAN2 [28] along with original ones for binary detection of facial images. **SeqDeepFake**: [63] dataset consists of 85k sequential manipulated face images based on two representative facial manipulation techniques, facial components manipulation [32] and facial attributes manipulation [27]. The labels include annotations of manipulation sequences with diverse sequence lengths. **R-splicer**: Augmenting real data by generating pseudo-fake images is a common practice in deepfake detection [36, 49, 11, 66, 87, 40]. Such methods simulate characteristic face-swap artefacts using simplistic operations on a predefined set of regions. In this work, we use a

⁴<https://openai.com/index/gpt-4v-system-card/>

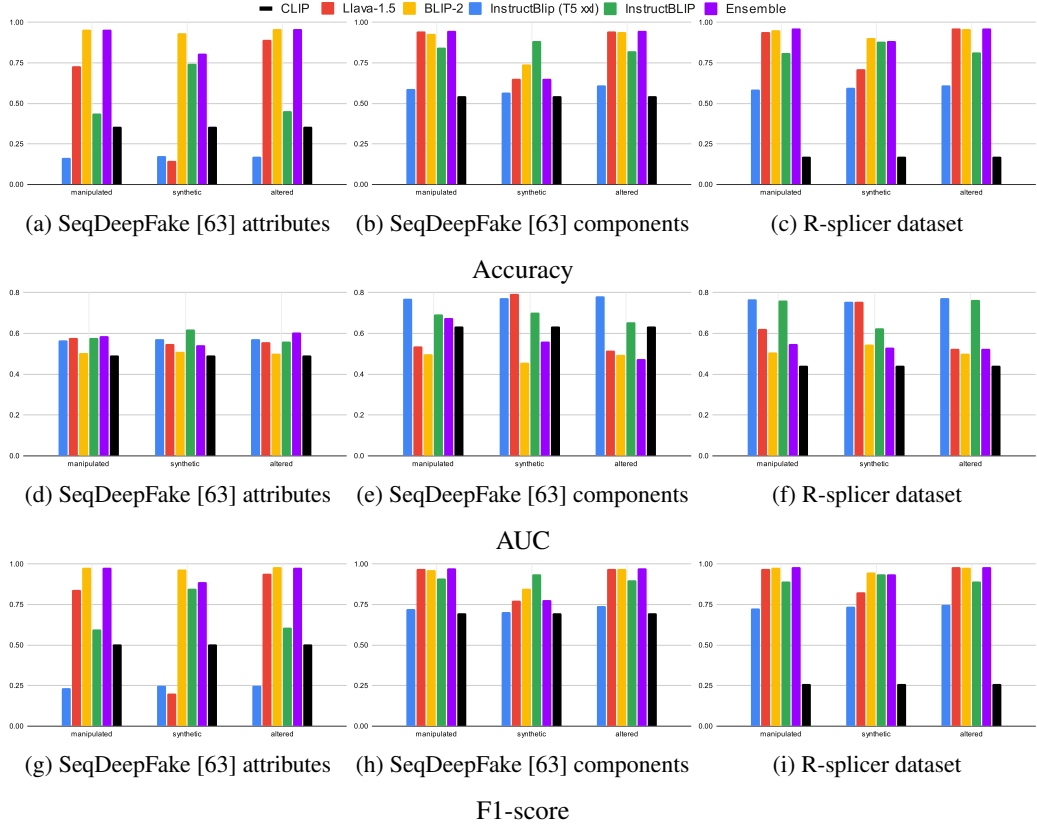


Figure 2: Exact Match (*EM*) Performance of each VLLM in terms of Accuracy (top), AUC (mid) and F1-score (bottom) for the top 3 synonyms “manipulated”, “synthetic” and “altered”

spliced dataset of 59k images to evaluate fine-grained labels of five regions –entire face, mouth, nose, eyes, eyebrows– as implemented by Mejri *et al.* [49].

4.3 Metrics

Accuracy and the Area Under the Receiver Operating Characteristics (ROC) Curve (**AUC**) are the most common metrics used in DeepFake detection [81, 52, 65]. However, as the datasets in the task are massively imbalanced, we also use the harmonic mean of Precision and Recall (**F1-score**) for the binary task. Furthermore, we note that as AUC is a measure of the classifier’s performance at different thresholds, it has very limited value in the VQA task where matching strategies result in polarised decisions; however, we include it for reference. In the fine-grained task, we use mean Average Precision (**mAP**), AUC and F1-score as indicators of classification performance.

5 Results

5.1 Binary Classification

Robustness to different prompts: We use seven synonyms for the positive class: “manipulated”, “deepfake”, “synthetic”, “altered”, “fabricated”, “face forgery” and “falsified”. As the binary task is simple and the instruction format is a ‘Yes’ or ‘No’ question, we use *EM* as a matching approach in this evaluation. In Fig. 2, we see the performance of each tested model under the binary detection setting on the two sub-sets of SeqDeepFake [63] and the R-splicer dataset using the three best performing synonyms: “manipulated”, “synthetic” and “altered”. The first observation is that no VLLM clearly outperforms others across all datasets and metrics. However, we see that BLIP-2 [35] has the most robust performance to the given instruction, even though it is the smallest in terms of parameters. Furthermore, the additional parameters of T5-xxl [13] do not seem to aid the task

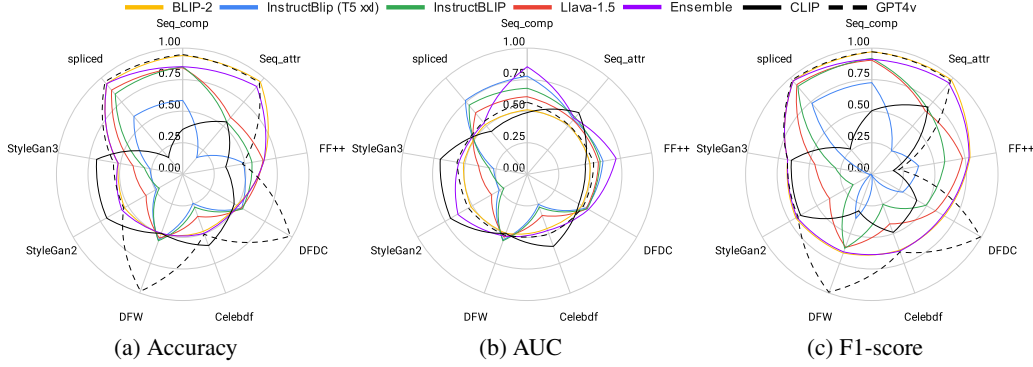


Figure 3: Exact Match (*EM*) Performance of each VLLM on all nine benchmarks

compared to the base InstructBLIP [15] with T5 generator, as the base model performs comparably better across most benchmarks. We theorise that as the VLLMs have not been explicitly trained on image-language pairs of manipulated images, a large number of parameters on the language generation leads to more hallucinations [25, 78] for this simple but abstract task. Compared to the CLIP [59], models appear to have competitive performance with the exception of InstructBLIP with T5xxl LLM. When both base models, i.e. BLIP-2 [35] and LlaVa [43], have relatively good performance, the ensemble shows marginal improvement, particularly in terms of Accuracy and F1; however, this is not consistent therefore we do not continue the investigation to fine-grained labels. The detailed performance of all models and synonyms across all datasets and additional analysis on CLIP [59] features can be found in the Appendix.

Overall model performance: We average the performance of the three best-performing synonyms on all nine benchmarks in Fig. 3. No model clearly outperforms others across all metrics and datasets; however, we can observe competitive performance from BLIP-2 [35] on the binary task, even though it is the smallest model in terms of parameters. We also see that all models struggle with the more challenging in-the-wild datasets, such as CelebDF [41], which highlights the need for further development to achieve adequate generalisation.

Vision Encoder Finetuning: We finetune contrastively the vision encoder of LlaVa on FF++ using a sigmoid loss [82] over an ensemble of prompts for the real/fake categories, and evaluate as described in the previous section. Training details for the vision encoder can be found in Appendix C. The architecture with the fine-tuned vision encoder shows improved within dataset and cross-dataset performance as shown in Tab. 1. Even without detailed captions or updating the LLM weights, we see there are still gains from a task specific vision encoder, particularly in terms of F1-score with an average improvement of nearly 4% within dataset and nearly 2% cross-dataset (for SeqDeepFake, CelebDF and StyleGAN2).

Table 1: Binary performance of LlaVa-1.5 [43] with a fine-tuned Vision Encoder against the zero-shot baseline.

	LlaVa Baseline		LlaVa w. fine-tuned Vision Encoder	
	Acc.	F1	Acc.	F1
FF++	64.54	73.10	64.57 (+0.03%)	76.83 (+3.73%)
SeqDeepfake Attr.	58.92	66.15	61.22 (+2.30%)	68.03 (+1.88%)
SeqDeepfake Comp.	84.62	90.57	84.24 (-0.37%)	90.20 (-0.38%)
R-Splicer	87.11	92.50	87.31 (+0.20%)	92.62 (+0.12%)
DFDC	54.02	58.24	53.86 (-0.16%)	58.65 (+0.41%)
CelebDF	35.67	41.81	37.60 (+1.93%)	43.53 (+1.72%)
DFW	53.35	61.56	53.45 (+0.10%)	61.90 (+0.34%)
StyleGAN2	33.67	38.62	35.20 (+1.53%)	39.72 (+1.10%)
StyleGAN3	39.80	45.66	39.30 (-0.50%)	45.74 (+0.08%)

Table 2: Model performance on open-ended fine-grained detection using a) *contains* and b) *CLIP* matching

	BLIP-2			InstructBLIP			InstructBLIP-xxl			LlaVa-1.5		
	mAP	AUC	F1	mAP	AUC	F1	mAP	AUC	F1	mAP	AUC	F1
SeqDeepFake [63] attributes	61.8	51.0	20.4	61.3	50.4	18.3	63.1	53.6	<u>37.5</u>	<u>61.7</u>	<u>51.1</u>	40.0
SeqDeepFake [63] components	59.5	50.5	14.7	<u>59.2</u>	<u>50.0</u>	4.1	60.2	51.8	26.2	59.0	49.6	<u>17.1</u>
R-Splicer	55.8	55.6	31.3	52.3	53.2	23.5	<u>53.8</u>	<u>54.0</u>	<u>31.1</u>	58.7	57.5	41.6

(a) Assessment of model performance during open-ended evaluation with *contains* distance matching.

	BLIP-2			InstructBLIP			InstructBLIP-xxl			LlaVa-1.5		
	mAP	AUC	F1	mAP	AUC	F1	mAP	AUC	F1	mAP	AUC	F1
SeqDeepFake [63] attributes	63.0	53.6	73.5	59.9	50.9	<u>74.0</u>	60.4	50.7	55.5	<u>61.0</u>	<u>51.3</u>	74.1
SeqDeepFake [63] components	<u>58.8</u>	<u>52.7</u>	<u>71.0</u>	55.5	49.0	71.7	59.9	55.7	59.8	56.1	49.6	71.7
R-Splicer	<u>54.3</u>	<u>55.3</u>	66.2	48.5	49.3	<u>66.5</u>	54.0	53.1	60.3	56.7	57.4	66.5

(b) Assessment of model performance during open-ended evaluation with *CLIP* distance matching.

Metrics: In terms of the selected metrics, following the initial intuition, there is limited information we can get from the standard Accuracy and AUC used in the binary task. Both are heavily skewed by the label distribution, which is typically imbalanced in deepfake datasets; however, the latter may also not be fit for VLLMs as AUC measures performance at different thresholds, which are not present with *EM* and *contains* matching strategies. As such, we argue that for the task at hand, the F1-score –and consequently robust to imbalance metrics– are more appropriate.

5.2 Finegrained Evaluation

For the fine-grained task, we evaluate the performance of the selected models in the open and closed vocabulary settings. The fine-grained labels are evaluated on samples where the ground truth is positive – i.e., on DeepFake samples.

Open-Ended VQA: We first evaluate the selected VLLMs under the open vocabulary VQA setting on the three fine-grained datasets. The results using *contains* and *CLIP distance* matching are reported in Tab. 2a and Tab. 2b respectively. An *EM* strategy is not possible in multi-label tasks, so no such evaluation is performed. No model clearly outperforms others across all metrics and datasets. In fact, we can observe that, in most cases, they have comparable performance. This holds true for both *contains* and *CLIP distance* metrics. In terms of matching strategy, using the *CLIP distance* consistently and greatly improves recall, as is evident by the improvement in the F1-score and explicitly shown in Appendix H. This matching approach slightly lowers the mAP and AUC scores compared to the *contains* metrics; however, using the cosine distance to match the open-ended responses to the class categories semantically may offer a more reliable output for the class of interest, as seen by the F1-score.

Multiple choice VQA: The performance of the VLLMs on the multiple-choice instruction is shown in Fig. 4. Even though the open-ended setting is theoretically more challenging, the performances of all tested models are comparable to each other and worse on the multiple-choice instruction for both mAP and AUC. Regarding the F1-score, however, LlaVa [43] consistently performs better than other models. Under the multiple-choice setting, we observe that the models tend to mention all label names, which raises the number of False Positives – a significant limitation of the multiple choice setting – or respond with “All of them” or “None of them”, which makes matching of any sort more challenging and is reflected even more in the lower F1 score. Appendix G includes detailed metrics for each category.

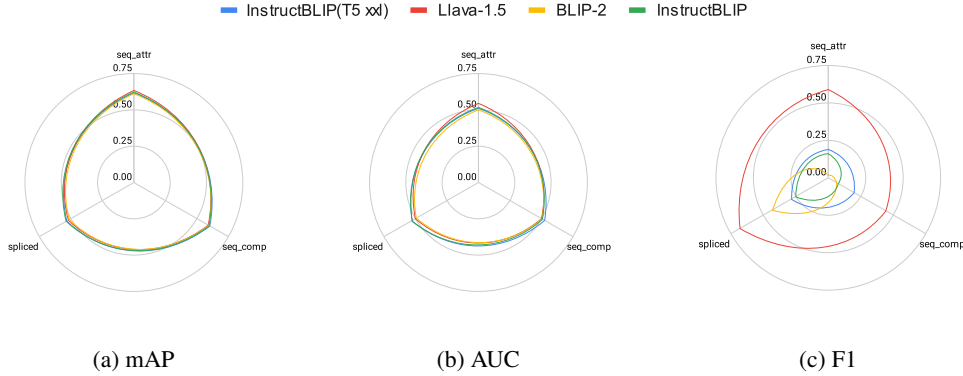


Figure 4: Assessment of model performance in multiple-choice settings, in terms of a) mAP, b) AUC and c) F1 during multiple-choice evaluation with *contains* matching.

Table 3: Open-ended qualitative evaluation with human annotators in Tab. a and BertScore [85] in Tab. b- d

Model	Human Eval. Score	Model	Precision	Recall	F1
BLIP-2	0.35	BLIP-2	79.77	78.75	79.24
InstructBLIP	0.36	InstructBLIP	86.53	<u>83.22</u>	84.81
InstructBLIP-xxl	0.33	InstructBLIP-xxl	80.73	<u>81.78</u>	81.25
LlaVa-1.5	0.38	LlaVa-1.5	<u>84.86</u>	85.31	85.08

(a) Average score of Human Evaluation (R-splicer)

Model	Precision	Recall	F1
BLIP-2	79.87	79.72	79.61
InstructBLIP	81.12	<u>83.89</u>	86.90
InstructBLIP-xxl	<u>82.57</u>	81.77	81.01
LlaVa-1.5	87.40	86.37	<u>85.39</u>

(b) SeqDeepFake [63] attributes

Model	Precision	Recall	F1
BLIP-2	79.55	79.76	80.04
InstructBLIP	83.47	<u>85.34</u>	87.39
InstructBLIP-xxl	82.53	81.87	81.23
LlaVa-1.5	85.94	86.33	<u>86.74</u>

(c) SeqDeepFake [63] components

(d) R-splice

5.3 Qualitative Evaluation

As the BertScore [85] is shown to correlate with human evaluation, we first present the Bert-score precision, recall, and F1 scores achieved by each model for the fine-grained open-ended responses compared with ground truth references that have been formatted using the prompt: “The areas that are $[s_i]$ are $[cls_i]$ ”. The results of this evaluation, along with the score of human annotators [19, 10] on a subset of the R-Splicer dataset, are shown in Tab. 3. As in previous sections, no model clearly outperforms others across all benchmarks; however, we see that LlaVa-1.5 [43] has the most competitive performance for most benchmarks, closely followed by InstructBLIP [15]. This is consistent with qualitative evaluations on VQA tasks [19, 44].

Overall performance: In the simpler binary setting, BLIP-2 is more robust to instruction than other models with more parameters; however, when it comes to fine-grained evaluation, larger models show an advantage in reasoning and identifying areas of manipulation in the open-ended and multiple-choice settings. It is, however, worth noting that no model clearly outperforms others across all metrics and datasets. All of the results presented are based on zero-shot evaluations, where models are tested without being specifically trained for deepfake detection. Despite this, the models are able to leverage a semantic mapping between language and visual input from their very vast pre-training, giving them an inherent concept of “real” versus “fake.” This capability suggests that these models possess some degree of understanding when it comes to identifying deepfakes. However, this general understanding falls far behind that of task-specific models. When we fine-tune the vision encoder, there is a notable improvement in performance. The vision-language models can better capture details and nuances in the input data, which enhances their deepfake detection capabilities. Nevertheless, due to the scarcity of high-quality captions and large-scale vision-language datasets tailored to deepfake detection, the improvements remain limited and only in the binary task. Overall,

addressing these limitations—by creating specialised datasets and foundation models—could lead to substantial advancements in this area.

Limitations and Future Work: As the models in this work are all evaluated under zero-shot settings, their performance is below that of purpose-build networks seen in previous works [81], particularly for more challenging in-the-wild datasets. This further highlights the need for task specific models and more fine-grained deepfake datasets, which is a key finding of the experiments conducted in this work. A significant limitation is the lack of detailed language descriptions in datasets, making qualitative evaluation harder. Additionally, current datasets lack fine-grained labels, restricting assessments of manipulations to pseudo-fakes and SeqDeepFake [63]. Furthermore, as both the pertaining and evaluation datasets are not unbiased, the performance of all VLLMs is susceptible to the bias of the datasets, which is not addressed in this or previous benchmarks [81]. Identifying these shortcomings is important for future works on the task, particularly as VLLMs gain traction.

6 Conclusion

In conclusion, our proposed benchmark has several contributions; first and foremost, we propose a method to transform deepfake detection into a VQA problem beyond binary classification to leverage common sense reasoning as an inherent explainability mechanism. We show how this can be achieved in both a multiple-choice and open-ended VQA—with the latter being the most important use-case for new and unknown face forgery methods. This approach is used to evaluate a multi-label problem that is not typical of classic VQA. By doing so, we can systematically and consistently evaluate the common sense reasoning capabilities of current and future VLLMs in fine-grained deepfake detection.

Our selection of metrics and matching strategies allows for a fair evaluation of the proposed task. In particular, we include metrics that are robust to imbalance in both the binary and multi-label fine-grained tasks. Even though VLLMs in a zero-shot evaluation do not outperform purpose-built methods, the generated responses include reasoning, therefore holding promise for significant contributions in explainable deepfake detection, confirming the initial motivation behind examining the use of such models for the task and understanding the current capabilities. Moreover, as this benchmark can be extended in terms of models and datasets, it allows for a systematic and fair comparison of new language generation methods for explainable deepfake detection.

Ethics statement: The authors of this paper acknowledge the crucial role of ethical considerations in AI research and development. Our dedication lies in upholding principles of fairness and impartiality. Recognising the societal implications of generative technology (including VLLMs), we commit to transparency by openly communicating our findings and advancements with the research community.

Acknowledgments and Disclosure of Funding

This work is supported by the Luxembourg National Research Fund, under the BRIDGES2021/IS/16353350/FaKeDeTeR, and by POST Luxembourg. Experiments were performed on the Luxembourg national supercomputer MeluXina. The authors gratefully acknowledge the LuxProvide teams for their expert support.

References

- [1] Madhav Agarwal, Rudrabha Mukhopadhyay, Vinay P Namboodiri, and CV Jawahar. Audio-visual face reenactment. In *Proceedings of the IEEE/CVF Winter Conference on Applications of Computer Vision*, 2023.
- [2] Arjun Akula, Soravit Changpinyo, Boqing Gong, Piyush Sharma, Song-Chun Zhu, and Radu Soricut. Crossvqa: Scalably generating benchmarks for systematically testing vqa generalization. In *Proceedings of the 2021 Conference on Empirical Methods in Natural Language Processing*, 2021.
- [3] Omar Mustafa Al-Janabi, Osamah Mohammed Alyasiri, and Elaf Ayyed Jebur. GPT-4 versus Bard and Bing: LLMs for Fake Image Detection. In *2023 3rd International Conference on Intelligent Cybernetics Technology & Applications (ICICyTA)*, December 2023.

- [4] Jean-Baptiste Alayrac, Jeff Donahue, Pauline Luc, Antoine Miech, Iain Barr, Yana Hasson, Karel Lenc, Arthur Mensch, Katherine Millican, Malcolm Reynolds, et al. Flamingo: a visual language model for few-shot learning. *Advances in neural information processing systems*, 2022.
- [5] Lisa Alazraki, Lluis Castrejon, Mostafa Dehghani, Fantine Huot, Jasper Uijlings, and Thomas Mensink. How (not) to ensemble lylms for vqa. *arXiv preprint arXiv:2310.06641*, 2023.
- [6] Stella Bounareli, Christos Tzelepis, Vasileios Argyriou, Ioannis Patras, and Georgios Tzimiropoulos. Hyperreenact: one-shot reenactment via jointly learning to refine and retarget faces. In *Proceedings of the IEEE/CVF International Conference on Computer Vision*, 2023.
- [7] Junyi Cao, Chao Ma, Taiping Yao, Shen Chen, Shouhong Ding, and Xiaokang Yang. End-to-end reconstruction-classification learning for face forgery detection. In *Proceedings of the IEEE/CVF Conference on Computer Vision and Pattern Recognition*, 2022.
- [8] You-Ming Chang, Chen Yeh, Wei-Chen Chiu, and Ning Yu. AntifakePrompt: Prompt-Tuned Vision-Language Models are Fake Image Detectors. *arXiv preprint arXiv:2310.17419*, November 2023.
- [9] Soravit Changpinyo, Piyush Sharma, Nan Ding, and Radu Soricut. Conceptual 12m: Pushing web-scale image-text pre-training to recognize long-tail visual concepts. In *Proceedings of the IEEE/CVF Conference on Computer Vision and Pattern Recognition*, pages 3558–3568, 2021.
- [10] Anthony Chen, Gabriel Stanovsky, Sameer Singh, and Matt Gardner. Mocha: A dataset for training and evaluating generative reading comprehension metrics. In *Proceedings of the 2020 Conference on Empirical Methods in Natural Language Processing (EMNLP)*, 2020.
- [11] Liang Chen, Yong Zhang, Yibing Song, Lingqiao Liu, and Jue Wang. Self-Supervised Learning of Adversarial Example: Towards Good Generalizations for Deepfake Detection. In *Proceedings of the IEEE/CVF Conference on Computer Vision and Pattern Recognition*, 2022.
- [12] Wei-Lin Chiang, Zhuohan Li, Zi Lin, Ying Sheng, Zhanghao Wu, Hao Zhang, Lianmin Zheng, Siyuan Zhuang, Yonghao Zhuang, Joseph E. Gonzalez, Ion Stoica, and Eric P. Xing. Vicuna: An open-source chatbot impressing gpt-4 with 90%* chatgpt quality, March 2023. URL <https://lmsys.org/blog/2023-03-30-vicuna/>.
- [13] Hyung Won Chung, Le Hou, Shayne Longpre, Barret Zoph, Yi Tay, William Fedus, Yunxuan Li, Xuezhi Wang, Mostafa Dehghani, Siddhartha Brahma, et al. Scaling instruction-finetuned language models. *arXiv preprint arXiv:2210.11416*, 2022.
- [14] Alessandro Conti, Enrico Fini, Massimiliano Mancini, Paolo Rota, Yiming Wang, and Elisa Ricci. Vocabulary-free image classification. *Advances in Neural Information Processing Systems*, 2023.
- [15] Wenliang Dai, Junnan Li, Dongxu Li, Anthony Meng Huat Tiong, Junqi Zhao, Weisheng Wang, Boyang Li, Pascale N Fung, and Steven Hoi. Instructblip: Towards general-purpose vision-language models with instruction tuning. *Advances in Neural Information Processing Systems*, 2023.
- [16] Audrey de Rancourt-Raymond and Nadia Smaili. The unethical use of deepfakes. *Journal of Financial Crime*, 2023.
- [17] Brian Dolhansky, Russ Howes, Ben Pflaum, Nicole Baram, and Cristian Canton Ferrer. The deepfake detection challenge (dfdc) preview dataset, 2019.
- [18] Niki Maria Fotinopoulou and Ioannis Patras. Emoclip: A vision-language method for zero-shot video facial expression recognition. In *2024 IEEE 18th International Conference on Automatic Face and Gesture Recognition (FG)*, pages 1–10. IEEE, 2024.
- [19] Simon Ging, Maria Alejandra Bravo, and Thomas Brox. Open-ended VQA benchmarking of vision-language models by exploiting classification datasets and their semantic hierarchy. In *The Twelfth International Conference on Learning Representations (ICLR)*, 2024.
- [20] Yash Goyal, Tejas Khot, Douglas Summers-Stay, Dhruv Batra, and Devi Parikh. Making the v in vqa matter: Elevating the role of image understanding in visual question answering. In *Proceedings of the IEEE conference on computer vision and pattern recognition*, 2017.
- [21] Ijaz Ul Haq, Khalid Mahmood Malik, and Khan Muhammad. Multimodal neurosymbolic approach for explainable deepfake detection. *ACM Transactions on Multimedia Computing, Communications and Applications*, 2023.

[22] Feijuan He, Yaxian Wang, Xianglin Miao, and Xia Sun. Interpretable visual reasoning: A survey. *Image and Vision Computing*, 2021.

[23] Edward J Hu, Phillip Wallis, Zeyuan Allen-Zhu, Yuanzhi Li, Shean Wang, Lu Wang, Weizhu Chen, et al. Lora: Low-rank adaptation of large language models. In *International Conference on Learning Representations*, 2021.

[24] Baojin Huang, Zhongyuan Wang, Jifan Yang, Jiaxin Ai, Qin Zou, Qian Wang, and Dengpan Ye. Implicit identity driven deepfake face swapping detection. In *Proceedings of the IEEE/CVF Conference on Computer Vision and Pattern Recognition*, 2023.

[25] Ziwei Ji, Nayeon Lee, Rita Frieske, Tiezheng Yu, Dan Su, Yan Xu, Etsuko Ishii, Ye Jin Bang, Andrea Madotto, and Pascale Fung. Survey of hallucination in natural language generation. *ACM Computing Surveys*, 2023.

[26] Shan Jia, Reilin Lyu, Kangran Zhao, Yize Chen, Zhiyuan Yan, Yan Ju, Chuanbo Hu, Xin Li, Baoyuan Wu, and Siwei Lyu. Can ChatGPT Detect DeepFakes? A Study of Using Multimodal Large Language Models for Media Forensics. *arXiv preprint arXiv:2403.14077*, March 2024. arXiv:2403.14077 [cs].

[27] Yuming Jiang, Ziqi Huang, Xingang Pan, Chen Change Loy, and Ziwei Liu. Talk-to-edit: Fine-grained facial editing via dialog. In *Proceedings of the IEEE/CVF International Conference on Computer Vision (ICCV)*, 2021.

[28] Tero Karras, Samuli Laine, Miika Aittala, Janne Hellsten, Jaakko Lehtinen, and Timo Aila. Analyzing and improving the image quality of stylegan. In *Proceedings of the IEEE/CVF Conference on Computer Vision and Pattern Recognition (CVPR)*, June 2020.

[29] Tero Karras, Miika Aittala, Samuli Laine, Erik Härkönen, Janne Hellsten, Jaakko Lehtinen, and Timo Aila. Alias-free generative adversarial networks. In *Advances in Neural Information Processing Systems*, 2021.

[30] Mamadou Keita, Wassim Hamidouche, Hassen Bougueffa, Abdenour Hadid, and Abdelmalik Taleb-Ahmed. Harnessing the power of large vision language models for synthetic image detection. *arXiv preprint arXiv:2404.02726*, 2024.

[31] Sohail Ahmed Khan and Duc-Tien Dang-Nguyen. CLIPping the Deception: Adapting Vision-Language Models for Universal Deepfake Detection. *arXiv preprint arXiv:2402.12927*, February 2024.

[32] Hyunsu Kim, Yunjey Choi, Junho Kim, Sungjoo Yoo, and Youngjung Uh. Exploiting spatial dimensions of latent in gan for real-time image editing. In *Proceedings of the IEEE Conference on Computer Vision and Pattern Recognition*, 2021.

[33] Ranjay Krishna, Yuke Zhu, Oliver Groth, Justin Johnson, Kenji Hata, Joshua Kravitz, Stephanie Chen, Yannis Kalantidis, Li-Jia Li, David A Shamma, et al. Visual genome: Connecting language and vision using crowdsourced dense image annotations. *International journal of computer vision*, 123:32–73, 2017.

[34] Chuqiao Li, Zhiwu Huang, Danda Pani Paudel, Yabin Wang, Mohamad Shahbazi, Xiaopeng Hong, and Luc Van Gool. A continual deepfake detection benchmark: Dataset, methods, and essentials. In *Proceedings of the IEEE/CVF Winter Conference on Applications of Computer Vision (WACV)*, January 2023.

[35] Junnan Li, Dongxu Li, Silvio Savarese, and Steven Hoi. Blip-2: Bootstrapping language-image pre-training with frozen image encoders and large language models. In *International Conference on Machine Learning*. PMLR, 2023.

[36] Lingzhi Li, Jianmin Bao, Ting Zhang, Hao Yang, Dong Chen, Fang Wen, and Baining Guo. Face X-Ray for More General Face Forgery Detection. In *Proceedings of the IEEE/CVF Conference on Computer Vision and Pattern Recognition*, 2020.

[37] Lingzhi Li, Jianmin Bao, Ting Zhang, Hao Yang, Dong Chen, Fang Wen, and Baining Guo. Face X-Ray for More General Face Forgery Detection. In *Proceedings of the IEEE/CVF Conference on Computer Vision and Pattern Recognition*, 2020.

[38] Linjie Li, Jie Lei, Zhe Gan, and Jingjing Liu. Adversarial vqa: A new benchmark for evaluating the robustness of vqa models. In *Proceedings of the IEEE/CVF International Conference on Computer Vision*, 2021.

[39] Rongjie Li, Yu Wu, and Xuming He. Learning by Correction: Efficient Tuning Task for Zero-Shot Generative Vision-Language Reasoning. In *Proceedings of the IEEE/CVF Conference on Computer Vision and Pattern Recognition*, April 2024.

[40] Yuezun Li and Siwei Lyu. Exposing deepfake videos by detecting face warping artifacts. *arXiv preprint arXiv:1811.00656*, 2018.

[41] Yuezun Li, Xin Yang, Pu Sun, Honggang Qi, and Siwei Lyu. Celeb-df: A large-scale challenging dataset for deepfake forensics. In *IEEE Conference on Computer Vision and Pattern Recognition (CVPR)*, 2020.

[42] Tsung-Yi Lin, Michael Maire, Serge Belongie, James Hays, Pietro Perona, Deva Ramanan, Piotr Dollár, and C Lawrence Zitnick. Microsoft coco: Common objects in context. In *Computer Vision–ECCV 2014: 13th European Conference, Zurich, Switzerland, September 6–12, 2014, Proceedings, Part V 13*, 2014.

[43] Haotian Liu, Chunyuan Li, Yuheng Li, and Yong Jae Lee. Improved baselines with visual instruction tuning, 2023.

[44] Haotian Liu, Chunyuan Li, Qingyang Wu, and Yong Jae Lee. Visual instruction tuning. In *Advances in Neural Information Processing Systems*, 2023.

[45] Zhian Liu, Maomao Li, Yong Zhang, Cairong Wang, Qi Zhang, Jue Wang, and Yongwei Nie. Fine-grained face swapping via regional gan inversion. In *Proceedings of the IEEE/CVF Conference on Computer Vision and Pattern Recognition*, 2023.

[46] Yuhang Lu and Touradj Ebrahimi. Towards the Detection of AI-Synthesized Human Face Images. *arXiv preprint arXiv:2402.08750*, February 2024.

[47] Jie Ma, Pinghui Wang, Dechen Kong, Zewei Wang, Jun Liu, Hongbin Pei, and Junzhou Zhao. Robust visual question answering: Datasets, methods, and future challenges. *IEEE Transactions on Pattern Analysis and Machine Intelligence*, 2024.

[48] Kenneth Marino, Mohammad Rastegari, Ali Farhadi, and Roozbeh Mottaghi. Ok-vqa: A visual question answering benchmark requiring external knowledge. In *Proceedings of the IEEE/cvf conference on computer vision and pattern recognition*, 2019.

[49] Nesryne Mejri, Enjie Ghorbel, and Djamila Aouada. UNTAG: Learning Generic Features for Unsupervised Type-Agnostic Deepfake Detection. In *ICASSP 2023 - 2023 IEEE International Conference on Acoustics, Speech and Signal Processing (ICASSP)*, 2023.

[50] Sachit Menon and Carl Vondrick. Visual Classification via Description from Large Language Models, December 2022. *arXiv:2210.07183 [cs]*.

[51] Anand Mishra, Shashank Shekhar, Ajeet Kumar Singh, and Anirban Chakraborty. Ocr-vqa: Visual question answering by reading text in images. In *2019 international conference on document analysis and recognition (ICDAR)*. IEEE, 2019.

[52] Dat Nguyen, Nesryne Mejri, Inder Pal Singh, Polina Kuleshova, Marcella Astrid, Anis Kacem, Enjie Ghorbel, and Djamila Aouada. Laa-net: Localized artifact attention network for high-quality deepfakes detection. In *Proceedings of the IEEE/CVF Conference on Computer Vision and Pattern Recognition*, 2024.

[53] Yunsheng Ni, Depu Meng, Changqian Yu, Chengbin Quan, Dongchun Ren, and Youjian Zhao. Core: Consistent representation learning for face forgery detection. In *Proceedings of the IEEE/CVF Conference on Computer Vision and Pattern Recognition*, pages 12–21, 2022.

[54] Alexander Quinn Nichol, Prafulla Dhariwal, Aditya Ramesh, Pranav Shyam, Pamela Mishkin, Bob McGrew, Ilya Sutskever, and Mark Chen. Glide: Towards photorealistic image generation and editing with text-guided diffusion models. In *International Conference on Machine Learning*. PMLR, 2022.

[55] James Oldfield, Christos Tzelepis, Yannis Panagakis, Mihalis Nicolaou, and Ioannis Patras. Parts of speech–grounded subspaces in vision-language models. *Advances in Neural Information Processing Systems*, 2024.

[56] Vicente Ordonez, Girish Kulkarni, and Tamara Berg. Im2text: Describing images using 1 million captioned photographs. *Advances in neural information processing systems*, 24, 2011.

[57] Yassine Ouali, Adrian Bulat, Brais Matinez, and Georgios Tzimiropoulos. Black box few-shot adaptation for vision-language models. In *Proceedings of the IEEE/CVF International Conference on Computer Vision*, 2023.

[58] Or Patashnik, Zongze Wu, Eli Shechtman, Daniel Cohen-Or, and Dani Lischinski. Styleclip: Text-driven manipulation of stylegan imagery. In *Proceedings of the IEEE/CVF International Conference on Computer Vision*, 2021.

[59] Alec Radford, Jong Wook Kim, Chris Hallacy, Aditya Ramesh, Gabriel Goh, Sandhini Agarwal, Girish Sastry, Amanda Askell, Pamela Mishkin, Jack Clark, et al. Learning transferable visual models from natural language supervision. In *International Conference on Machine Learning*. PMLR, 2021.

[60] Andreas Rössler, Davide Cozzolino, Luisa Verdoliva, Christian Riess, Justus Thies, and Matthias Nießner. FaceForensics++: Learning to detect manipulated facial images. In *International Conference on Computer Vision (ICCV)*, 2019.

[61] Christoph Schuhmann, Richard Vencu, Romain Beaumont, Robert Kaczmarczyk, Clayton Mullis, Aarush Katta, Theo Coombes, Jenia Jitsev, and Aran Komatsuzaki. Laion-400m: Open dataset of clip-filtered 400 million image-text pairs. *arXiv preprint arXiv:2111.02114*, 2021.

[62] Dustin Schwenk, Apoorv Khandelwal, Christopher Clark, Kenneth Marino, and Roozbeh Mottaghi. A-ovqa: A benchmark for visual question answering using world knowledge. In *European Conference on Computer Vision*, pages 146–162. Springer, 2022.

[63] Rui Shao, Tianxing Wu, and Ziwei Liu. Detecting and recovering sequential deepfake manipulation. In *European Conference on Computer Vision (ECCV)*, 2022.

[64] Piyush Sharma, Nan Ding, Sebastian Goodman, and Radu Soricut. Conceptual captions: A cleaned, hypernymed, image alt-text dataset for automatic image captioning. In *Proceedings of the 56th Annual Meeting of the Association for Computational Linguistics (Volume 1: Long Papers)*, pages 2556–2565, 2018.

[65] Yichen Shi, Yuhao Gao, Yingxin Lai, Hongyang Wang, Jun Feng, Lei He, Jun Wan, Changsheng Chen, Zitong Yu, and Xiaochun Cao. SHIELD : An Evaluation Benchmark for Face Spoofing and Forgery Detection with Multimodal Large Language Models. *arXiv preprint arXiv:2402.04178*, February 2024.

[66] Kaede Shiohara and Toshihiko Yamasaki. Detecting deepfakes with self-blended images. In *Proceedings of the IEEE/CVF Conference on Computer Vision and Pattern Recognition*, 2022.

[67] Oleksii Sidorov, Ronghang Hu, Marcus Rohrbach, and Amanpreet Singh. Textcaps: a dataset for image captioning with reading comprehension. In *Computer Vision–ECCV 2020: 16th European Conference, Glasgow, UK, August 23–28, 2020, Proceedings, Part II* 16, 2020.

[68] Michał Stypułkowski, Konstantinos Vougioukas, Sen He, Maciej Zięba, Stavros Petridis, and Maja Pantic. Diffused heads: Diffusion models beat gans on talking-face generation. In *Proceedings of the IEEE/CVF Winter Conference on Applications of Computer Vision (WACV)*, January 2024.

[69] Ke Sun, Shen Chen, Taiping Yao, Haozhe Yang, Xiaoshuai Sun, Shouhong Ding, and Rongrong Ji. Towards General Visual-Linguistic Face Forgery Detection. *arXiv preprint arXiv:2307.16545*, February 2024.

[70] Dídac Surís, Sachit Menon, and Carl Vondrick. Vipergrpt: Visual inference via python execution for reasoning. *Proceedings of IEEE International Conference on Computer Vision (ICCV)*, 2023.

[71] Loc Trinh, Michael Tsang, Sirisha Rambhatla, and Yan Liu. Interpretable and trustworthy deepfake detection via dynamic prototypes. In *Proceedings of the IEEE/CVF Winter Conference on Applications of Computer Vision (WACV)*, 2021.

[72] Yabin Wang, Zhiwu Huang, Zhiheng Ma, and Xiaopeng Hong. Linguistic profiling of deepfakes: An open database for next-generation deepfake detection. *arXiv preprint arXiv:2401.02335*, 2024.

[73] Alexandros Xenos, Niki Maria Fotleinopoulou, Ioanna Ntinou, Ioannis Patras, and Georgios Tzimiropoulos. VLLMs Provide Better Context for Emotion Understanding Through Common Sense Reasoning. *arXiv:2404.07078 [cs]*, April 2024.

[74] Weihao Xia, Yujiu Yang, Jing-Hao Xue, and Baoyuan Wu. Tedigan: Text-guided diverse face image generation and manipulation. In *Proceedings of the IEEE/CVF Conference on Computer Vision and Pattern Recognition*, 2021.

[75] Peng Xu, Wenqi Shao, Kaipeng Zhang, Peng Gao, Shuo Liu, Meng Lei, Fanqing Meng, Siyuan Huang, Yu Qiao, and Ping Luo. Lvlm-ehub: A comprehensive evaluation benchmark for large vision-language models. *arXiv preprint arXiv:2306.09265*, 2023.

[76] Yuting Xu, Jian Liang, Gengyun Jia, Ziming Yang, Yanhao Zhang, and Ran He. TALL: Thumbnail Layout for Deepfake Video Detection. In *2023 IEEE/CVF International Conference on Computer Vision (ICCV)*, Paris, France, October 2023. IEEE.

[77] Zipeng Xu, Enver Sangineto, and Nicu Sebe. Stylerdalle: Language-guided style transfer using a vector-quantized tokenizer of a large-scale generative model. In *Proceedings of the IEEE/CVF International Conference on Computer Vision*, 2023.

[78] Ziwei Xu, Sanjay Jain, and Mohan Kankanhalli. Hallucination is Inevitable: An Innate Limitation of Large Language Models. *arXiv:2401.11817 [cs]*, January 2024.

[79] Zhiyuan Yan, Yong Zhang, Yanbo Fan, and Baoyuan Wu. Ucf: Uncovering common features for generalizable deepfake detection. In *Proceedings of the IEEE/CVF International Conference on Computer Vision (ICCV)*, October 2023.

[80] Zhiyuan Yan, Yong Zhang, Yanbo Fan, and Baoyuan Wu. Ucf: Uncovering common features for generalizable deepfake detection. In *Proceedings of the IEEE/CVF International Conference on Computer Vision*, 2023.

[81] Zhiyuan Yan, Yong Zhang, Xinhang Yuan, Siwei Lyu, and Baoyuan Wu. DeepfakeBench: A Comprehensive Benchmark of Deepfake Detection. In *Advances in Neural Information Processing Systems*, 2023.

[82] Xiaohua Zhai, Basil Mustafa, Alexander Kolesnikov, and Lucas Beyer. Sigmoid loss for language image pre-training. In *Proceedings of the IEEE/CVF International Conference on Computer Vision*, pages 11975–11986, 2023.

[83] Kai Zhang, Lingbo Mo, Wenhui Chen, Huan Sun, and Yu Su. Magicbrush: A manually annotated dataset for instruction-guided image editing. *Advances in Neural Information Processing Systems*, 36, 2024.

[84] Susan Zhang, Stephen Roller, Naman Goyal, Mikel Artetxe, Moya Chen, Shuohui Chen, Christopher Dewan, Mona Diab, Xian Li, Xi Victoria Lin, et al. Opt: Open pre-trained transformer language models. *arXiv preprint arXiv:2205.01068*, 2022.

[85] Tianyi Zhang*, Varsha Kishore*, Felix Wu*, Kilian Q. Weinberger, and Yoav Artzi. Bertscore: Evaluating text generation with bert. In *International Conference on Learning Representations*, 2020.

[86] Cairong Zhao, Chutian Wang, Guosheng Hu, Haonan Chen, Chun Liu, and Jinhui Tang. Istvt: Interpretable spatial-temporal video transformer for deepfake detection. *IEEE Transactions on Information Forensics and Security*, 2023.

[87] Tianchen Zhao, Xiang Xu, Mingze Xu, Hui Ding, Yuanjun Xiong, and Wei Xia. Learning self-consistency for deepfake detection. In *Proceedings of the IEEE/CVF International Conference on Computer Vision*, 2021.

[88] Bojia Zi, Minghao Chang, Jingjing Chen, Xingjun Ma, and Yu-Gang Jiang. Wilddeepfake: A challenging real-world dataset for deepfake detection. In *Proceedings of the 28th ACM International Conference on Multimedia*, 2020.

[89] Dragos-Constantin Tăntăru, Elisabeta Oneață, and Dan Oneață. Weakly-supervised deepfake localization in diffusion-generated images. In *Proceedings of the IEEE/CVF Winter Conference on Applications of Computer Vision*, 2024.

Appendix

A Model Zoo

LlaVa-1.5 [43] is an extension of the LlaVa [44] model. We use the variant with CLIP-ViT-L-14 as a vision encoder and Vicuna-7b [12] language model. **BLIP-2** [35] uses a QFormer architecture to bridge frozen language and vision encoders. We use the variant with CLIP-ViT-L-14 as a vision encoder and the 2.7b OPT [84] language model. **InstructBLIP** [15] is a family of VLLMs that exploits the basic BLIP-2 [35] architecture and advances the task by giving the instruction to both the QFormer and the LLM. We use two variants of the architecture, with two different LLMs from the T5 family [13]; in the base architecture, we use the CLIP-ViT-L-14 as a vision encoder and the T5-xl LLM. **InstructBLIPxxl** uses the same vision encoder and the T5-xxl language model. A comparison of all architectures in terms of parameters and pre-training datasets can be seen in Tab. 4. It is worth noting, that none of the pre-training datasets are related to deepfakes, making the task more challenging. For the **ensemble**, we chose BLIP-2 [35] and LlaVa-15 [43], based of two main factors: a) they show the most competitive performance on most datasets as seen in Fig. 3 and b) they have the least overlap in terms of pre-training data thus we intuitively expect them having complementary information. The ensembling method adopted in this work is using score fusion with majority voting; in the occasions where the models disagree, the mean is taken. **GPT4v** is used for comparison in the binary tasks, however as the training details of this model are unknown, it should only be treated as an upper bound.

Architecture	FLOPS	# Params	Pre-training Data
BLIP-2 [35]	$0.38T$	$3.74B$	COCO [42], Visual Genome [33], CC3M [64], CC12M [9], SBU [56], and $115M$ images from the LAION400M [61]
InstructBLIP [15]	$0.33T$	$4.02B$	COCO [42], WebCapFilt [35], TextCaps [67], VQAv2 [20], OK-VQA [48], AOK-VQA [62], OCR-VQA [51], LLaVA-Instruct-150K [44]
InstructBLIP-xxl [15]	$0.53T$	$12.31B$	COCO [42], WebCapFilt [35], TextCaps [67], VQAv2 [20], OK-VQA [48], AOK-VQA [62], OCR-VQA [51], LLaVA-Instruct-150K [44]
LlaVa-1.5 [43]	$4.14T$	$7.06B$	LLaVA-Instruct-150K [44], VQAv2 [20], OK-VQA [48], OCR-VQA [51]

Table 4: Comparisons of model FLOPS, number of parameters and pre-training datasets for selected VLLMs

Implementation Details. All experiments were conducted using four NVIDIA A100 GPUs, with 40GB of memory. We use the PyTorch deep learning framework for all model evaluation tasks and weights published on HuggingFace⁵.

B Binary Classification Prompts

The term deepfake is a colloquial term for a wide range of manipulations using generative models, from altering one small area all the way to fully generated images and videos. As such, the class name itself has several synonyms that can describe it. To assess the model’s robustness to instruction, we first prompt an LLM –specifically ChatGPT3.5 to give us synonyms for a deepfake. This is done as an automation step to incorporate the general consensus into the method without the author’s bias, following previous works [50]. The following synonyms are tested for the positive class: “manipulated”, “deepfake”, “synthetic”, “altered”, “fabricated”, “face forgery” and “falsified”. We show the detailed performance of all models on all synonyms in Tab. 6. To provide context, we also provide the cross-dataset performance of several discriminative SOTA works in Tab. 5. The models show the most consistent performance on synonyms “manipulated”, “synthetic” and “altered”; therefore, we do all subsequent analyses on these prompts.

⁵<https://huggingface.co/>

Table 5: Reported cross-dataset performance of purpose-built discriminative SoTA models.

	CelebDF [41]		DFW [88]		DFDC [17]	
	AUC	mAP	AUC	mAP	AUC	mAP
UCF [80]	82.40	-	-	-	80.50	-
X-Ray [37]	79.50	-	-	-	65.50	-
Xception [60]	61.18	66.93	65.29	55.37	69.90	91.98
REECE [7]	70.93	70.35	68.16	54.41	-	-
CORE [53]	74.28	-	-	-	73.41	-
LAA-Net [52]	86.28	91.93	57.13	56.89	69.69	93.67

C Vision Encoder Fine-tuning

We fine-tune the CLIP-L/14-336 Vision encoder using LoRA [23] adaptors. Specifically, we add 32 adaptors to the queries, keys, values and out projection of the attention heads, with an alpha of 32, a dropout rate of 0.2 and 4bit quantization. As the available datasets lack sample level descriptions, we use the text embeddings of the synonyms for the positive category and the embeddings of “real”, “original”, “unaltered”, “authentic”, “legitimate”, “genuine”, “bona fide” for the negative. We apply a Sigmoid loss over the cosine similarity [82] of all relevant text embeddings in the batch and train the vision encoder for 50 epochs. The updated weights are then used in the LLaVa-1.5 architecture.

D CLIP Embeddings

As most models use CLIP [59] variants as backbone vision encoders, we assess the separability of samples in real and manipulated images in each dataset by visualising them in a two-dimensional plane using t-SNE. The resulting visualisations can be seen in Fig. 5. The samples appear more separable in some datasets. Interestingly, the StyleGAN datasets, where the images are fully generated, seem to have more distinguishable latent representations from real images. The separability is not necessarily reflected in the language generation as seen in Sec. 5.1; to further examine the root cause of this, we first calculate the average image embedding of each class so as to create a class prototype and retrieve the top-10 nearest language token embeddings, seen in Tab. 8. The first observation that can be made is that none of the tokens seems related to the task at hand, which would potentially inform prompt selection, so without the reasoning capabilities of the LLM, the token retrieval on its own is not very informative. Secondly, we see that a number of tokens are repeated across datasets and for both classes, which can be attributed to the much smaller sub-space of the deepfake task compared to the CLIP latent space; so, while the image embeddings are somewhat separable for several datasets retrieving the nearest language tokens shows that the subspace is not very much related to face forgery. From these two observations, we can better understand the zero-shot performance of the tested foundation models. Finally, we show the performance of CLIP on the binary classification task in Tab. 7. We use an ensemble of prompts using the Imagenet prompt templates [59]; for the positive class, we average the embeddings of the prompts for synonyms “manipulated”, “synthetic” and “altered”; for the negative, we use “real”, “original” and “unaltered”. Contrary to previous VQA works [14, 19] that use CLIP retrieval as an upper bound, we see this is not the case in the task. This can be attributed to the more abstract definition of the class in the deepfake detection task, as well as the pre-training dataset, which is more object-oriented.

E Human Evaluation

The human evaluation is based upon previous studies in VQA evaluation [19, 10]. The humans are asked to rate model predictions on a scale from 1 to 5, where 1 is completely wrong and 5 is completely correct.

Evaluation dataset: We use a subset of the pseudo-fake R-Splicer dataset for the human evaluation study, as it has artefacts visible to the human eye and is thus easier for the annotators to assess the response quality.

Table 6: Binary Performance of tested models

Synonym	Seq. Deepfake Attr.			Seq. Deepfake Comp.			R-Splicer	FF++			DFDC			CelebDF			DFW			StyleGAN2			StyleGAN3				
	Acc.	AUC	F1	Acc.	AUC	F1	Acc.	AUC	F1	Acc.	AUC	F1	Acc.	AUC	F1	Acc.	AUC	F1	Acc.	AUC	F1	Acc.	AUC	F1			
manipulated	95.36	50.49	97.62	94.44	50.46	97.14	95.32	50.59	97.60	65.42	49.76	79.00	49.47	49.95	66.13	52.20	49.87	68.34	50.40	49.99	66.93	52.60	50.25	68.69	50.00	49.29	66.33
altered	96.06	50.25	97.99	94.62	49.93	97.23	95.85	50.22	97.88	65.76	50.01	79.24	49.50	49.98	66.21	51.60	49.31	67.73	50.37	49.96	66.94	53.20	50.84	69.13	51.49	50.76	67.67
synthetic	95.48	51.75	97.68	93.95	52.09	96.87	90.45	54.42	94.95	65.27	51.63	78.15	49.46	49.93	65.95	40.80	39.20	56.21	50.51	50.17	65.05	54.60	52.37	69.53	53.73	53.05	68.37
deepfake	93.02	51.54	96.86	93.15	54.50	96.43	89.47	54.91	94.40	64.66	52.19	77.28	49.35	49.82	65.81	39.40	37.79	55.24	50.48	50.16	64.18	53.80	51.53	69.16	50.75	50.07	66.23
fabricated	95.00	51.80	97.43	94.02	50.56	96.92	91.70	52.53	95.65	64.79	50.58	78.04	49.41	49.89	66.03	46.60	44.64	62.66	50.85	50.49	65.80	53.80	51.51	69.24	51.49	50.80	67.01
face forgery	96.11	49.98	98.01	94.72	51.87	97.28	94.18	51.18	97.00	65.03	50.42	78.36	49.44	49.92	66.01	53.00	50.69	68.79	49.67	49.27	66.19	53.60	51.26	69.51	51.49	50.76	67.66
falsified	95.58	52.10	97.73	93.29	51.74	96.52	92.03	53.25	95.83	65.42	51.46	78.38	49.40	49.88	65.94	42.80	41.07	58.55	52.92	52.56	67.06	53.80	51.57	68.99	52.99	52.30	68.02

(a) BLIP-2 [35] performance on the nine benchmark datasets.

Synonym	Seq. Deepfake Attr.			Seq. Deepfake Comp.			R-Splicer	FF++			DFDC			CelebDF			DFW			StyleGAN2			StyleGAN3				
	Acc.	AUC	F1	Acc.	AUC	F1	Acc.	AUC	F1	Acc.	AUC	F1	Acc.	AUC	F1	Acc.	AUC	F1	Acc.	AUC	F1	Acc.	AUC	F1			
manipulated	43.85	57.87	59.50	84.34	69.39	91.25	80.95	76.04	89.17	53.87	60.01	54.01	55.11	54.90	41.78	19.40	19.95	9.84	58.73	58.68	61.10	17.40	18.05	5.49	26.12	26.25	19.51
altered	45.10	55.92	60.86	82.10	65.58	89.91	81.31	76.41	89.40	54.32	61.01	53.83	55.51	55.29	42.39	19.40	19.94	10.24	58.37	58.32	61.23	17.80	18.41	6.80	27.61	27.70	23.62
synthetic	74.33	61.92	84.97	88.39	57.01	92.67	88.14	62.50	75.18	59.24	54.51	69.10	44.20	42.93	56.61	51.54	51.23	64.65	29.60	28.99	38.25	38.06	37.86	45.75			
deepfake	20.19	58.62	29.42	62.94	75.23	75.93	66.76	78.77	79.26	49.04	60.62	39.09	53.54	53.17	24.19	26.80	28.13	0.54	59.07	59.30	43.77	26.80	28.13	0.54	28.36	28.74	4.00
fabricated	74.23	58.01	84.96	90.68	63.74	97.97	91.92	57.64	95.76	62.85	50.97	75.76	52.18	52.42	61.59	55.80	53.82	69.26	51.35	51.03	65.02	28.60	27.87	38.77	32.84	32.53	44.44
face forgery	19.90	58.47	28.99	54.55	74.75	68.60	71.10	82.75	82.42	51.26	62.73	42.42	54.76	54.42	30.14	26.80	28.13	0.54	56.81	57.03	41.85	27.00	28.32	1.08	32.84	33.29	4.26
falsified	19.62	58.33	28.55	57.76	75.13	71.51	64.94	81.28	77.80	49.44	61.70	38.24	54.15	53.80	27.19	26.00	27.29	0.54	55.86	56.14	34.03	26.00	27.29	0.54	29.10	29.52	2.06

(b) InstructBLIP [15] performance on the nine benchmark datasets.

Synonym	Seq. Deepfake Attr.			Seq. Deepfake Comp.			R-Splicer	FF++			DFDC			CelebDF			DFW			StyleGAN2			StyleGAN3				
	Acc.	AUC	F1	Acc.	AUC	F1	Acc.	AUC	F1	Acc.	AUC	F1	Acc.	AUC	F1	Acc.	AUC	F1	Acc.	AUC	F1	Acc.	AUC	F1			
manipulated	16.44	56.68	23.57	58.88	77.04	72.42	58.49	76.85	72.63	48.53	60.88	36.70	53.88	53.54	28.75	24.80	26.05	0.00	54.09	54.37	32.36	24.80	26.05	0.00	25.37	25.74	1.96
altered	17.21	57.08	24.80	60.98	78.14	74.19	60.99	77.24	74.72	49.04	61.25	37.78	53.99	53.66	29.59	23.40	24.52	1.54	54.90	55.15	36.37	23.20	24.33	1.03	38.81	39.39	0.00
synthetic	17.40	57.18	25.11	56.64	77.17	70.42	59.76	75.42	73.74	49.74	61.62	39.46	53.79	53.44	27.57	24.00	25.21	0.54	56.85	57.06	43.52	24.20	25.40	0.52	28.36	28.74	4.00
deepfake	7.98	52.29	8.77	13.43	54.42	16.24	41.08	69.28	56.04	42.22	56.31	22.40	52.28	51.85	14.48	35.06	36.76	0.00	51.36	51.73	13.75	35.06	36.76	0.00	38.81	39.39	0.00
fabricated	21.06	59.07	22.72	64.34	79.91	76.92	64.97	77.75	77.90	51.71	62.81	43.75	54.40	54.08	31.55	23.80	24.96	1.04	56.00	56.13	48.37	23.60	24.77	0.52	25.37	25.74	1.96
face forgery	9.42	53.04	11.47	30.63	63.48	42.46	41.83	69.76	56.84	42.83	56.74	23.90	52.24	51.82	16.20	34.20	35.92	0.00	51.66	52.02	15.64	34.20	35.92	0.00	26.87	27.25	2.00
falsified	16.73	56.83	24.04	58.74	78.28	72.25	63.55	78.75	76.76	49.68	61.77	38.94	53.81	53.47	28.49	24.40	25.57	1.56	54.25	54.49	35.95	24.00	25.19	0.52	26.87	27.25	2.00

(c) InstructBLIP [15] with Flan-T5-xxl [13] language model performance on the nine benchmark datasets.

Synonym	Seq. Deepfake Attr.			Seq. Deepfake Comp.			R-Splicer	FF++			DFDC			CelebDF			DFW			StyleGAN2			StyleGAN3				
	Acc.	AUC	F1	Acc.	AUC	F1	Acc.	AUC	F1	Acc.	AUC	F1	Acc.	AUC	F1	Acc.	AUC	F1	Acc.	AUC	F1	Acc.	AUC	F1			
manipulated	73.05	57.79	84.14	94.34	53.56	97.07	94.05	62.20	96.90	67.52	55.20	79.18	54.51	54.80	64.63	38.80	37.47	52.78	52.92	52.58	66.54	37.40	36.13	51.17	47.01	46.61	61.62
altered	89.16	55.64	92.22	94.30	51.65	97.06	96.10	52.45	98.01	66.42	51.41	79.42	50.67	51.11	65.95	49.00	46.85	65.31	51.05	50.65	67.17	47.20	45.12	63.74	50.75	50.04	66.67
synthetic	14.54	54.96	20.09	65.21	79.44	77.79	71.17	56.30	76.74	59.67	50.67	60.69	44.14	59.86	56.70	39.69	37.54	60.24	23.90	39.67	51.74	16.40	17.19	0.95	21.64	21.86	8.70
deepfake	8.00	52.16	8.29	38.46	67.52	51.91	51.03	74.43	65.99	46.16	59.25	31.44	54.18	53.79	23.32	34.66	36.33	0.61	53.63	53.98	20.52	34.20	35.92	0.00	37.31	37.88	0.00
fabricated	12.72	54.31	16.93	58.11	75.38	71.73	66.03	78.94	78.70	51.93	63.19	47.05	54.18	54.38	31.04	25.00	26.24	0.53	53.82	54.07	33.94	25.00	26.24	0.53	29.85	30.19	9.62
face forgery	12.62	54.56	16.72	56.78	76.25	70.50	71.86	84.60	82.94	55.75	66.12	50.36	56.38	56.35	37.71	29.40	30.79										

Table 7: CLIP baseline performance on the binary task of the nine selected benchmarks.

Dataset	Accuracy	AUC	F1
SeqDeepFake attributes [63]	54.62	63.46	69.63
SeqDeepFake components [63]	35.80	49.10	50.38
R-splice	17.14	44.33	25.98
FF++ [60]	34.85	46.50	17.38
DFDC [17]	46.84	46.75	40.93
CelebDF [41]	59.80	60.95	49.11
DFW [88]	49.67	49.90	31.09
StyleGan2 [28].	69.20	69.92	65.16
StyleGan3 [29]	69.40	69.63	64.35

Table 8: Top 10 closest tokens to the class prototypes. Unique to the class tokens are in **bold**.

Dataset	Original	DeepFake
SeqDeepFake attributes	natives, labeling, liz, saving , rink, demon , pitch, creole, godis, wentz	natives, liz, labeling, rink, wentz, ronda , godis, creole, %), melissa
SeqDeepFake components	natives, labeling , qld, romo, liz, creole , dhoni , , hijab , gaining	natives, qld, liz, gaining, romo, %), cuomo , klo , minions , cowgirl
R-splice	natives, wentz, anglo, liz, %), qld, anca, romo , ronda , ural	anglo, %), wentz, liz, natives, klo , anca, qld, ural, weed
FF++	natives, qld, wentz, anglo, cuomo, anca, liz, labeling , romo, melissa	natives, qld, wentz, anglo, liz, cuomo, anca, %), weed , romo
DFDC	natives, wentz, anglo, liz, ronda, qld, %), anca, romo, !!	anglo, wentz, natives, liz, %), ronda, qld, anca, !!, romo
CelebDF	natives, liz, wentz, ronda , %), anglo, qld, romo, labeling , anca	anglo, natives, ural , klo , creole , %), weed , wentz, romo, minions
DFW	anglo, %), ronda, wentz, ural, natives, liz, klo , rene, ator	anglo, natives, ural , klo , creole , %), weed , wentz, romo, minions
StyleGan2	natives, liz, wentz, ronda, %), anglo , qld, romo, labeling, anca	anglo, natives, ural , wentz , ator, ronda , klo , anca, qld
StyleGan3	natives, liz, wentz, ronda, romo, labeling, aa , anca , %), ural	natives, labeling, liz, rink , ronda, romo, creole , melissa, wentz, saving

[44] as well–, we note that larger models attempt to provide a justification for their response, which is ultimately the goal of investigating VLLMs for this task.

As the available datasets lack sample specific descriptions of manipulation areas, we include BertScore of the tested VLLMs on the MagicBrush [83] dataset to assess response quality on the neighbouring task of image editing detection, that is language driven in table Tab. 9.

G Multiple-choice VQA

Further to the analysis in Sec. 5.2, we show the performance of all models on the multiple-choice VQA setting in Tab. 10. In the multiple-choice setting, all models have comparable mAP and AUC, however, LlaVa-1.5 [43] shows a clear advantage in terms of Recall and F1.

H Open-ended VQA

The detailed performance of each model on the open-ended fine-grained detection can be seen on Tabs. 11 to 14. The matching strategy has a significant impact on Recall, as mentioned in Sec. 5.2, thus also increasing the F1 score.

Table 9: BertScore of selected VLLMs on MagicBrush dataset

	Precision	Recall	F1
Blip	85.44	84.37	84.57
InstructBlip	84.56	85.09	84.82
InstructBlip-xxl	81.07	84.55	81.88
LlaVa 1.5	83.08	84.77	83.87

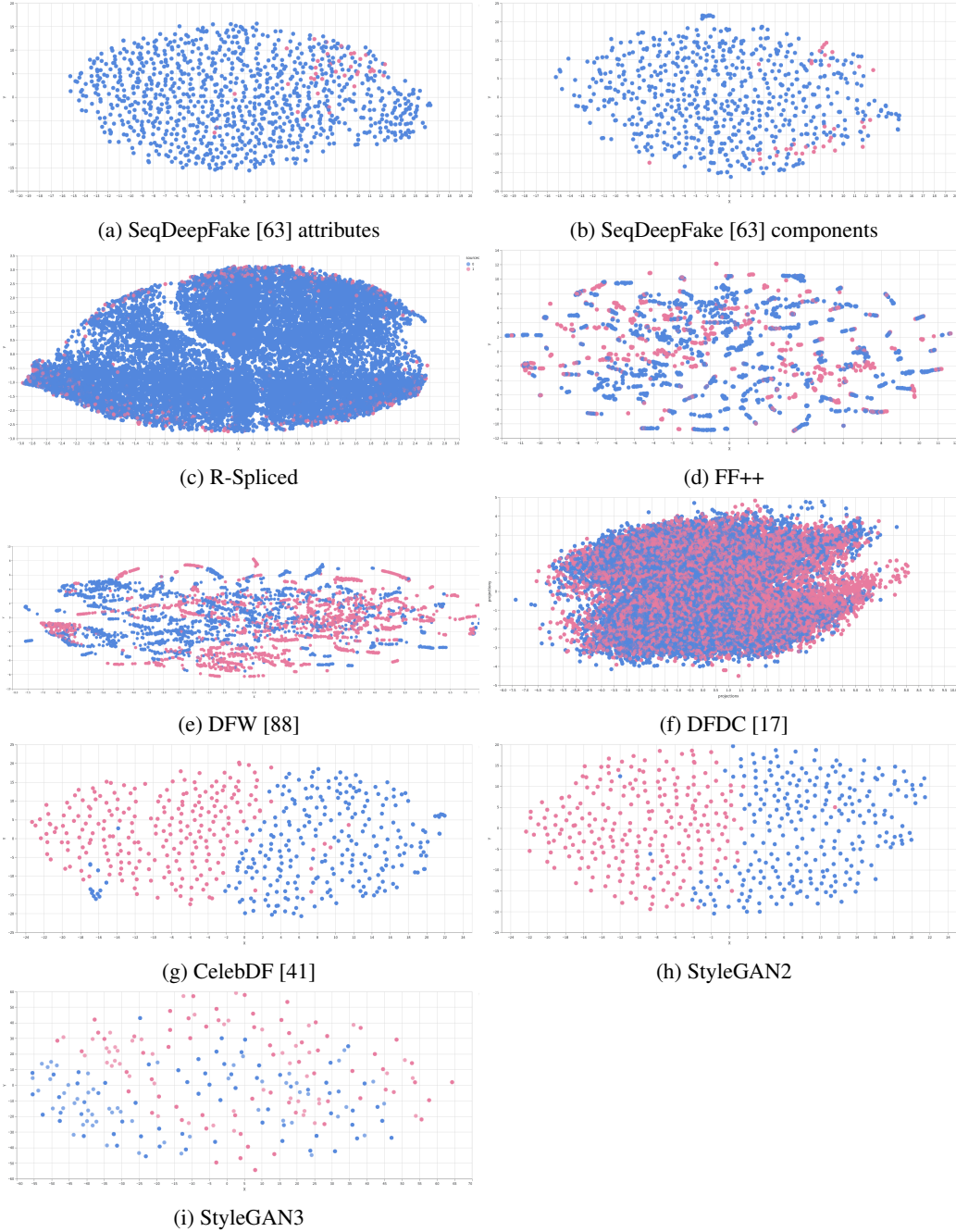


Figure 5: t-SNE Visualisation of CLIP [59] image embeddings on the test set of the selected datasets (perplexity=50)

Qualitative evaluation

The aim of the study is to understand how well the generated responses reflect the ground truth i.e. how well each model can spot the manipulated areas.

The possible manipulation areas are: entire face (faceswap), mouth, nose, eyes, eyebrows. Each model is instructed to "Explain briefly what areas of this image are manipulated?".

See the image, the correct answer and the predicted answers. Select the score that best reflects how closely the predicted answers capture the same information as the correct answer. This means that the statements should be semantically similar but do not need to match the class names exactly.

1. completely wrong
2. mostly wrong
3. half right
4. mostly right
5. completely right

The entire evaluation should take 30-60 mins.

(a) Annotator Briefing

The areas that are manipulated are: eyebrows mouth faceswap



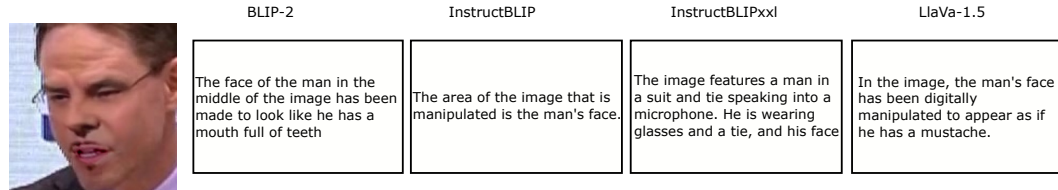
The eyes of the man in the hat

1 2 3 4 5

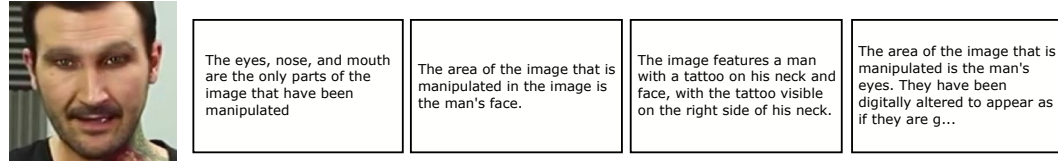
completely wrong completely correct

(b) Annotation Form

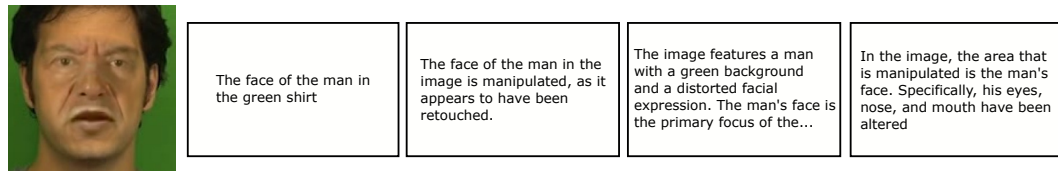
Figure 6: Example of Briefing(a) and Annotation Form(b) shown to human evaluators.



(a) Ground Truth: Mouth, Faceswap



(b) Ground Truth: Eyebrows, Eyes



(c) Ground Truth: Nose, Mouth, Faceswap

Figure 7: Samples of generated responses in an open-ended setting.

Table 10: Performance of tested VLLMs in multiple-choice setting

	AUC	F1	mAP	Recall		AUC	F1	mAP	Recall		AUC	F1	mAP	Recall
Bangs	49.8	0.0	60.3	0.0	nose	50.0	0.0	55.4	0.0	nose	51.3	46.9	52.5	42.2
Eyeglasses	49.9	8.0	63.4	4.6	eye	50.8	10.2	66.8	5.5	eyebrows	50.4	57.0	52.0	63.1
Beard	49.8	1.0	61.0	0.5	eyebrow	51.0	11.0	58.3	6.0	eyes	50.2	56.2	51.5	61.9
Smiling	50.0	0.0	58.3	0.0	lip	50.0	0.0	67.6	0.0	mouth	49.9	45.4	51.9	40.9
Young	50.0	0.0	62.3	0.0	hair	50.4	9.7	48.9	5.4	faceswap	44.6	9.2	50.2	5.5
Total	49.9	4.5	61.1	2.5	Total	50.4	10.3	59.4	5.7	Total	49.3	42.9	51.6	42.7

(a) SeqDeepFake attributes [63]

(b) SeqDeepFake comp [63]

(c) R-Splicer

BLIP-2 [35]

	AUC	F1	mAP	Recall		AUC	F1	mAP	Recall		AUC	F1	mAP	Recall
Bangs	50.2	1.0	60.4	0.5	nose	50.0	0.0	55.4	0.0	nose	56.5	38.5	56.2	30.4
Eyeglasses	58.4	51.3	68.0	41.6	eye	52.2	11.7	67.7	6.5	eyebrows	52.5	58.0	53.1	66.5
Beard	50.0	0.3	61.0	0.2	eyebrow	50.6	3.3	58.2	1.7	eyes	52.6	16.5	53.1	10.1
Smiling	50.0	0.0	58.3	0.0	lip	50.0	0.0	67.6	0.0	mouth	52.9	13.0	54.3	7.1
Young	50.4	29.0	62.6	21.4	hair	51.1	24.7	49.3	23.6	faceswap	50.0	0.0	51.6	0.0
Total	51.8	20.4	62.1	15.9	Total	50.8	13.2	59.6	10.6	Total	52.9	31.5	53.7	28.5

(d) SeqDeepFake attributes [63]

(e) SeqDeepFake comp [63]

(f) R-Splicer

InstructBLIP [15]

	AUC	F1	mAP	Recall		AUC	F1	mAP	Recall		AUC	F1	mAP	Recall
Bangs	50.4	18.5	60.7	13.2	nose	50.0	0.0	55.4	0.0	nose	53.4	59.0	53.6	64.6
Eyeglasses	54.3	75.9	65.7	90.3	eye	57.3	39.1	70.3	31.2	eyebrows	52.7	31.5	53.3	22.9
Beard	50.0	0.1	61.0	0.1	eyebrow	54.4	21.0	60.8	13.0	eyes	51.0	8.5	52.0	4.7
Smiling	50.0	0.0	58.3	0.0	lip	50.0	0.0	67.6	0.0	mouth	57.0	41.6	56.5	32.3
Young	50.0	0.0	62.3	0.0	hair	50.1	38.4	48.8	44.4	faceswap	50.0	1.2	51.6	0.6
Total	50.9	31.5	61.6	34.5	Total	52.4	32.8	60.6	29.5	Total	52.8	28.4	53.4	25.0

(g) SeqDeepFake attributes [63]

(h) SeqDeepFake comp [63]

(i) R-Splicer

InstructBLIP [15] with T5-xxl [13] LLM

	AUC	F1	mAP	Recall		AUC	F1	mAP	Recall		AUC	F1	mAP	Recall
Bangs	52.2	38.1	61.4	27.3	nose	50.0	3.2	55.4	1.7	nose	49.6	67.6	51.6	98.2
Eyeglasses	58.2	73.0	67.5	77.8	eye	48.8	76.2	65.9	91.0	eyebrows	50.1	67.9	51.8	98.4
Beard	57.1	74.3	64.7	86.7	eyebrow	49.2	71.8	57.4	96.0	eyes	50.2	67.7	51.5	98.9
Smiling	54.7	36.4	61.1	25.2	lip	49.5	3.8	67.5	2.0	mouth	50.0	68.0	51.9	98.4
Young	49.5	74.1	62.1	92.6	hair	52.2	65.4	49.9	94.9	faceswap	50.4	68.2	51.8	99.8
Total	54.3	59.2	63.3	61.9	Total	49.9	44.1	59.2	57.1	Total	50.1	67.9	51.7	98.7

(j) SeqDeepFake attributes [63]

(k) SeqDeepFake comp [63]

(l) R-Splicer

LlaVa-1.5 [43]

Table 11: BLIP-2 [35] performance with *contains* and *CLIP* matching in open-ended VQA

	AUC	F1	mAP	Recall		AUC	F1	mAP	Recall
Bangs	53.9	33.7	62.5	22.2	Bangs	56.0	73.5	64.1	99.9
Eyeglasses	56.4	40.3	67.0	28.0	Eyeglasses	60.0	75.9	69.6	99.9
Beard	50.1	2.1	61.1	1.1	Beard	59.9	74.1	66.8	99.9
Smiling	49.9	1.0	58.3	0.5	Smiling	50.2	72.0	56.4	99.9
Young	44.6	24.9	60.3	18.2	Young	51.6	75.1	61.2	100.0
Total	51.0	20.4	61.8	14.0	Total	55.5	74.1	63.6	99.9

 (a) SeqDeepFake attributes [63] with *contains* matching (b) SeqDeepFake attributes [63] with *CLIP* matching

	AUC	F1	mAP	Recall		AUC	F1	mAP	Recall
nose	49.4	20.1	55.2	13.2	nose	51.6	69.0	54.8	100.0
eye	50.1	10.5	66.6	6.0	eye	49.8	77.3	64.1	99.8
eyebrow	49.9	2.2	57.7	1.1	eyebrow	50.4	70.9	55.7	100.0
lip	50.6	11.6	68.0	6.5	lip	50.0	78.2	66.2	100.0
hair	52.6	29.3	50.3	19.8	hair	49.7	63.2	46.8	99.8
Total	50.5	14.7	59.5	9.3	Total	50.3	71.7	57.5	99.9

 (c) SeqDeepFake comp. [63] with *contains* matching

 (d) SeqDeepFake comp. [63] with *CLIP* matching

	AUC	F1	mAP	Recall		AUC	F1	mAP	Recall
nose	55.8	31.6	55.9	20.5	nose	54.4	66.6	58.5	99.9
eyebrows	50.4	2.5	52.0	1.2	eyebrows	51.7	66.6	52.7	99.9
eyes	54.0	37.3	53.7	27.8	eyes	53.5	66.3	53.7	100.0
mouth	52.7	20.5	53.7	12.4	mouth	52.8	66.8	54.1	100.0
faceswap	66.0	64.4	62.5	60.3	faceswap	55.1	66.4	57.1	100.0
Total	55.8	31.3	55.6	24.5	Total	53.5	66.5	55.2	100.0

 (e) R-splicer with *contains* matching

 (f) R-splicer with *CLIP* matching

Table 12: InstructBLIP [15] performance with *contains* and *CLIP* matching in open-ended VQA

	AUC	F1	mAP	Recall		AUC	F1	mAP	Recall
Bangs	51.3	9.1	61.1	5.2	Bangs	49.6	73.6	58.5	99.6
Eyeglasses	50.5	3.0	63.7	1.6	Eyeglasses	47.2	75.7	60.5	99.1
Beard	50.2	1.2	61.1	0.6	Beard	58.0	73.9	64.7	99.3
Smiling	50.0	1.2	58.3	0.6	Smiling	49.2	72.0	56.0	99.5
Young	50.0	76.8	62.3	99.9	Young	50.5	74.9	60.0	99.5
Total	50.4	18.3	61.3	21.6	Total	50.9	74.0	59.9	99.4

(a) SeqDeepFake attributes [63] with *contains* matching (b) SeqDeepFake attributes [63] with *CLIP* matching

	AUC	F1	mAP	Recall		AUC	F1	mAP	Recall
nose	50.1	0.9	55.5	0.4	nose	49.2	69.0	52.0	99.9
eye	50.0	0.1	66.4	0.1	eye	46.9	77.3	61.7	99.8
eyebrow	50.0	0.0	57.7	0.0	eyebrow	49.5	70.8	54.1	99.9
lip	49.7	0.4	67.5	0.2	lip	49.5	78.2	63.6	99.9
hair	50.4	18.8	49.0	16.4	hair	49.6	63.3	46.1	99.9
Total	50.0	5.1	59.2	4.3	Total	48.9	71.7	55.5	99.9

(c) SeqDeepFake comp. [63] with *contains* matching

(d) SeqDeepFake comp. [63] with *CLIP* matching

	AUC	F1	mAP	Recall		AUC	F1	mAP	Recall
nose	54.0	16.8	55.2	9.3	nose	50.8	66.6	52.0	99.9
eyebrows	50.4	3.3	52.1	1.7	eyebrows	49.2	66.6	49.3	99.9
eyes	50.4	9.3	51.6	5.4	eyes	49.9	66.3	49.2	99.9
mouth	53.0	19.4	54.0	11.8	mouth	51.0	66.8	51.0	100.0
faceswap	53.5	68.7	53.4	96.4	faceswap	41.3	66.4	45.3	100.0
Total	52.3	23.5	53.2	24.9	Total	48.5	66.5	49.3	99.9

(e) R-splicer with *contains* matching

(f) R-splicer with *CLIP* matching

Table 13: InstructBLIP [15] with T5-xxl LLM [13] performance, with *contains* and *CLIP* matching in open-ended VQA

	AUC	F1	mAP	Recall		AUC	F1	mAP	Recall
Bangs	54.4	27.4	62.9	16.7	Bangs	45.8	46.3	56.2	40.7
Eyeglasses	60.6	65.6	69.1	59.7	Eyeglasses	56.1	65.3	65.7	65.9
Beard	51.0	6.3	61.6	3.3	Beard	55.0	60.3	63.4	59.2
Smiling	51.9	11.5	59.5	6.2	Smiling	46.3	55.0	54.7	56.0
Young	50.0	76.8	62.3	100.0	Young	50.2	50.6	61.9	43.7
Total	53.6	37.5	63.1	37.2	Total	50.7	55.5	60.4	53.1

(a) SeqDeepFake attributes [63] with *contains* matching (b) SeqDeepFake attributes [63] with *CLIP* matching

	AUC	F1	mAP	Recall		AUC	F1	mAP	Recall
nose	50.1	0.9	55.5	0.4	nose	54.8	56.2	56.7	56.6
eye	50.0	0.1	66.4	0.1	eye	58.2	57.7	68.5	49.4
eyebrow	50.0	0.0	57.7	0.0	eyebrow	51.2	56.1	55.1	56.8
lip	49.7	0.4	67.5	0.2	lip	60.1	71.9	70.7	76.4
hair	50.4	18.8	49.0	16.4	hair	54.1	57.3	48.3	70.4
Total	50.0	5.1	59.2	4.3	Total	55.6	59.8	59.9	61.9

(c) SeqDeepFake comp. [63] with *contains* matching (d) SeqDeepFake comp. [63] with *CLIP* matching

	AUC	F1	mAP	Recall		AUC	F1	mAP	Recall
nose	53.1	18.4	54.0	10.6	nose	53.5	57.2	53.5	63.7
eyebrows	50.5	7.5	52.1	4.0	eyebrows	52.7	59.1	51.9	69.6
eyes	52.1	38.5	52.5	29.9	eyes	51.4	57.2	50.7	66.0
mouth	53.7	29.4	54.2	19.2	mouth	54.3	62.2	53.7	78.3
faceswap	59.5	61.9	57.1	63.7	faceswap	58.0	65.7	55.5	90.1
Total	53.8	31.1	54.0	25.5	Total	54.0	60.3	53.1	73.5

(e) R-splicer with *contains* matching

(f) R-splicer with *CLIP* matching

Table 14: LlaVa-1.5 [43] performance, with *contains* and *CLIP* matching in open-ended VQA

	AUC	F1	mAP	Recall		AUC	F1	mAP	Recall
Bangs	48.9	56.9	59.9	55.9	Bangs	46.4	73.5	56.9	99.9
Eyeglasses	53.6	39.0	65.2	27.4	Eyeglasses	51.9	75.9	65.9	100.0
Beard	52.5	16.7	62.5	9.5	Beard	57.9	74.1	64.0	100.0
Smiling	51.1	12.1	59.0	7.1	Smiling	52.7	72.0	59.2	100.0
Young	49.3	75.3	62.0	96.1	Young	47.5	75.1	58.8	100.0
Total	51.1	40.0	61.7	39.2	Total	51.3	74.1	61.0	100.0

(a) SeqDeepFake attributes [63] with *contains* matching (b) SeqDeepFake attributes [63] with *CLIP* matching

	AUC	F1	mAP	Recall		AUC	F1	mAP	Recall
nose	48.8	19.7	54.9	12.7	nose	51.9	68.9	53.6	99.9
eye	49.7	3.2	66.4	1.6	eye	50.0	77.4	63.1	100.0
eyebrow	49.9	7.1	57.7	3.8	eyebrow	48.7	70.8	54.1	100.0
lip	50.3	12.3	67.8	6.8	lip	50.8	78.2	65.3	100.0
hair	49.3	43.2	48.4	43.9	hair	46.8	63.3	44.5	100.0
Total	49.6	17.1	59.0	13.8	Total	49.6	71.7	56.1	100.0

(c) SeqDeepFake comp. [63] with *contains* matching

(d) SeqDeepFake comp. [63] with *CLIP* matching

	AUC	F1	mAP	Recall		AUC	F1	mAP	Recall
nose	57.6	34.8	57.4	22.5	nose	56.8	66.6	60.0	100.0
eyebrows	53.5	19.5	54.3	11.2	eyebrows	54.5	66.6	56.2	100.0
eyes	57.4	43.2	56.2	33.3	eyes	56.5	66.3	56.0	100.0
mouth	55.9	36.7	55.8	25.6	mouth	55.0	66.8	55.6	100.0
faceswap	68.8	73.8	63.6	84.6	faceswap	60.7	66.4	59.3	100.0
Total	58.7	41.6	57.4	35.5	Total	56.7	66.5	57.4	100.0

(e) R-splicer with *contains* matching

(f) R-splicer with *CLIP* matching